

Characterization of fluid transport properties of reservoirs using induced microseismicity

S.A. Shapiro, E. Rothert, V. Rath and J. Rindschwentner¹

keywords: permeability, hydraulic diffusivity, induced microseismicity, 3-D mapping

ABSTRACT

We systematically describe an approach to estimate the large scale permeability of reservoirs using seismic emission (microseismicity) induced by fluid injection. We call this approach the Seismicity Based Reservoir Characterization (SBRC). A simple variant of the approach is based on the hypothesis that the triggering front of the hydraulic-induced microseismicity propagates like a diffusive process (the pore pressure relaxation) in an effective homogeneous anisotropic poroelastic fluid-saturated medium. The permeability tensor of this effective medium is the permeability tensor upscaled to the characteristic size of the seismically-active heterogeneous rock volume. We show that in a homogeneous medium the surface of the seismicity triggering front has the same form as the group-velocity surface of the low-frequency anisotropic second-type Biot's wave (i.e. slow wave). Further, we generalize the SBRC for a 3-D mapping of the permeability tensor of heterogeneous reservoirs and aquifers. For this an approach similar to the geometrical optics approximation was derived and an equation describing kinematical aspects of triggering front propagation in a way similar to the eikonal equation for seismic wavefronts is used. In the case of isotropic heterogeneous media the inversion for the hydraulic properties of rocks follows from a direct application of this equation. We demonstrate the method on several field examples and test the approach on numerical models.

INTRODUCTION

The characterization of fluid-transport properties of rocks is one of the most important and difficult problems of reservoir geophysics. Active seismic methods have fundamental difficulties in estimating fluid mobility or the permeability tensor (see e.g., Shapiro and Mueller 1999). On the other hand, it would be highly attractive to use seismic methods to characterize hydraulic properties of rocks because of their large

¹email: shapiro@geophysik.fu-berlin.de, rothert@geophysik.fu-berlin.de

penetration distances and a potentially high resolution.

Here we describe and demonstrate an approach that combines the above mentioned advantages of seismic methods with an excellent potential to provide in-situ estimates of the permeability tensor. The corresponding permeability estimates characterize reservoirs on the large spatial scale of the order of $10^2 m - 10^3 m$. This approach (we call it SBRC: Seismicity Based Reservoir Characterization) uses a spatio-temporal analysis of fluid-injection induced microseismicity to reconstruct the permeability tensor (see Shapiro et al., 1997, 1998, 1999 and Audigane, 2000; see also the recent discussion Cornet 2000 and Shapiro et al. 2000). Such a microseismicity can be released by perturbations of the pore pressure caused by a fluid injection into rocks (e.g., fluid tests in boreholes). Evidently, the triggering of microearthquakes occur in some locations where rocks are in a near-failure equilibrium. Such locations can be just randomly distributed in the medium.

Recently, Shapiro et al. (1999) proposed to interpret the spatio-temporal evolution of the clouds of such microseismic events in terms of pore-pressure relaxation in media with anisotropic hydraulic diffusivity. They derived an equation for the microseismicity triggering front in homogeneous anisotropic poroelastic media. The propagation of the triggering front is controlled directly by the permeability tensor. Using this equation Shapiro et al. (1999) proposed a variant of the SBRC method, which considers real heterogeneous rocks as an effective homogeneous anisotropic poroelastic fluid-saturated medium. The permeability tensor of this effective medium is the permeability tensor upscaled to the characteristic size of the seismically active region.

In this paper we propose a technique to characterize heterogeneous distributions of the permeability in reservoirs. Firstly we give a theoretical introduction into SBRC for homogeneous anisotropic poroelastic media. We show that in a homogeneous medium the microseismicity-triggering front has the form of the group-velocity surface of the anisotropic diffuse wave of the pore-pressure relaxation (which is the low-frequency Biot-slow wave). Then we describe the concept of the SBRC approach to the 3-D mapping of hydraulic diffusivity. A differential equation is derived which approximately describes kinematics of the microseismicity triggering front in the case of quasi harmonic pore pressure perturbation. This approximation is similar to the geometrical optics approach for seismic waves. The propagation of the triggering front is considered in an intermediate asymptotic frequency range. This means that we assume that the dominant frequency of pressure perturbations is much smaller than the critical Biot frequency. On the other hand we assume, that the slow-wave dominant wavelength is smaller than the characteristic size of the heterogeneity of the hydraulic diffusivity. Then we suggest an algorithm of hydraulic diffusivity mapping in 3D in

the both cases, quasi-harmonic and quasi-step-function medium excitation. Finally we demonstrate the SBRC method on some case studies.

THE CONCEPT OF TRIGGERING FRONTS

In the following we approximate a real configuration of a fluid injection in a borehole by a point source of pore pressure perturbation in an infinite heterogeneous anisotropic poroelastic fluid-saturated medium. In the low-frequency limit of the Biot equations (Biot 1962) the pore-pressure perturbation p can be approximately described by the following differential equation of diffusion:

$$\frac{\partial p}{\partial t} = \frac{\partial}{\partial x_i} \left[D_{ij} \frac{\partial}{\partial x_j} p \right], \quad (1)$$

where D_{ij} are components of the tensor of the hydraulic diffusivity, x_j ($j = 1, 2, 3$) are the components of the radius vector from the injection point to an observation point in the medium and t is the time. This equation corresponds to the second-type Biot waves (the slow P-waves) in the low frequency limit and describes linear relaxation of pore-pressure perturbations. Note, that this equation is valid for a heterogeneous medium in respect of its hydraulic properties. In other words, components of the tensor of the hydraulic diffusivity can be heterogeneously distributed in the medium. The tensor of hydraulic diffusivity is directly proportional to the tensor of permeability (see e.g. Rindschwenter et al. within this volume).

In some situations (e.g., some hydrofracturing experiments) the hydraulic diffusivity can be changed considerably by the fluid injection. This means, that in the equation above the diffusivity tensor must become pore-pressure dependent. Therefore, this equation becomes non-linear. Such changes of the diffusivity take place in restricted regions around boreholes. However, our method is aimed at estimating the effective hydraulic diffusivity in a large rock volume of the spatial scale of the order of 1km.

Moreover, in a given elementary volume of the medium, the triggering of the earliest microseismic events starts before the substantial relaxation of the pore-pressure occurs. This means, that even in the 'near zone' very early events occur in the practically unchanged medium. In other words, the front of significant changes of the medium propagates behind the quicker triggering front of earlier microseismic events. However, it is precisely these early events that are important for our approach for estimating the diffusivity. Thus, the corresponding estimate should be approximately equal to the diffusivity of the unchanged medium even in such situations, where the diffusivity was strongly enhanced by the hydraulic fracturing. Because of this reason we assume that changes of the diffusivity caused by the injection can be neglected.

Thus, D_{ij} is assumed to be pressure independent in eq. (1).

To introduce the concept of triggering fronts let us firstly recall the form of the solution of (1) in the case of a homogeneous poroelastic medium. In the case of anisotropic homogeneous medium equation (1) takes the following form

$$\frac{\partial p}{\partial t} = D_{ij} \frac{\partial}{\partial x_i} \frac{\partial}{\partial x_j} p. \quad (2)$$

If the medium is also isotropic (i.e., $D_{11} = D_{22} = D_{33} = D$, and $D_{ij} = 0$, if $i \neq j$), then

$$\frac{\partial p}{\partial t} = D \Delta p, \quad (3)$$

and D is the scalar hydraulic diffusivity. If a time-harmonic perturbation $p_0 \exp(-i\omega t)$ of the pore-pressure perturbation is given on a small spherical surface of the radius a with the center at the injection point, then the solution of equations (3) is

$$p(r, t) = p_0 e^{-i\omega t} \frac{a}{r} \exp \left[(i-1)(r-a) \sqrt{\frac{\omega}{2D}} \right], \quad (4)$$

where ω is the angular frequency and $r = |\mathbf{r}|$ is the distance from the injection point to the point, where the solution is looked for. From equation (4) we note that the solution can be considered as a spherical wave (it corresponds to the slow compressional wave in the Biot theory) with the attenuation coefficient equal to $\sqrt{\omega/2D}$ and the slowness equal to $1/\sqrt{\omega 2D}$.

In reality the pore pressure at the injection point is not a harmonic function. Let us roughly approximate the pore pressure perturbation at the injection point by a step function $p(t) = p_0$, if $t \geq 0$ and $p(t) = 0$ if $t < 0$. For instance, this can be a rough approximation in some cases of a borehole fluid injection (e.g. for a hydraulic fracturing or other fluid tests). In a given elementary volume of the medium located at the distance $r = |\mathbf{r}|$ from the injection source, the triggering of microseismic events starts just before the substantial relaxation of the pore pressure has been reached. For a particular seismic event at the time t_0 the time evolution of the injection signal for the time $t > t_0$ is of no relevance for this event anymore. Thus, this event is triggered by the rectangular signal $p(t) = p_0$ if $0 \leq t \leq t_0$ and $p(t) = 0$ if $t < 0$ or $t > t_0$. The power spectrum of this signal has the dominant part in the frequency range below $2\pi/t_0$ (note that the choice of this frequency is of partially heuristic character; see the related discussions in Shapiro et al., 1997 and 1999). Thus, the probability, that this event was triggered by signal components from the frequency range $\omega \leq \pi/t_0$ is high. This probability for the lower energetic high frequency components is small. However, the propagation velocity of high-frequency components is higher than those of the low frequency components (see eq. 4). Thus, to a given time t_0 it is probable

that events will occur at distances, which are smaller than the travel distance of the slow-wave signal with the dominant frequency $2\pi/t_0$. The events are characterized by a significantly lower probability for larger distances. The spatial surface which separates these two spatial domains we call the triggering front.

Triggering fronts in homogeneous anisotropic media

Let us firstly assume, that the medium is homogeneous and isotropic. Then the slowness of the slow wave (see eq. 4) can be used to estimate the above mentioned size of the spatial domain, where microseismic events are characterized by a high probability. We obtain (see also Shapiro et al. 1997)

$$r = \sqrt{4\pi Dt}. \quad (5)$$

This is the equation for the triggering front in an effective isotropic homogeneous poroelastic medium with the scalar hydraulic diffusivity D .

With a correctly selected value of the hydraulic diffusivity, equation (5) corresponds to the upper bound of the cloud of events in the plot of their spatio-temporal distribution (i.e., the plot of r versus t). In Figure 1a such a spatio-temporal distribution of the microseismicity is shown for the the microseismic data collected in December 1983 during the hydraulic injection into crystalline rock at a depth of 3463 meters at the Fenton Hill (USA) geothermal energy site (see for details and further references Fehler et al., 1998). We see a good agreement between the theoretical curve with $D = 0.17 m^2/s$ and the data.

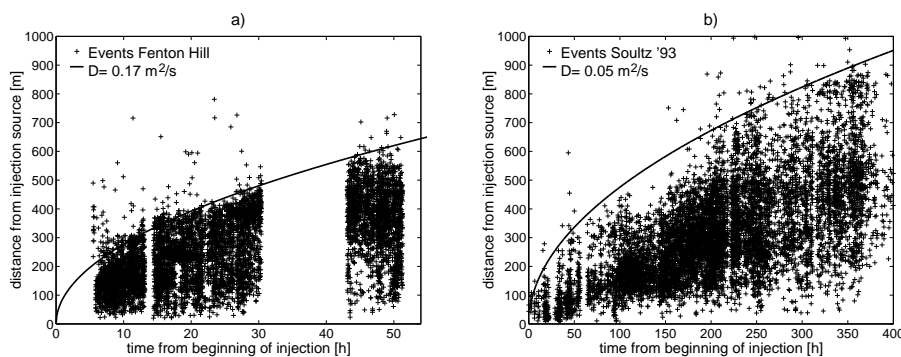


Figure 1: Distances of events from the injection source versus their occurrence time for a) the Fenton Hill experiment, 1983 and b) the Soultz-sous-Forets experiment, 1993

Such a good agreement supporting the above concept of the triggering of microseismicity can be observed in many other cases. For example Figure 1b shows

a similar plot for the Soultz-sous-Forêts experiment in 1993 in France, where about 9000 events were localized during the injection (see Dyer et al., 1994). The diffusivity $D = 0.05 m^2/s$ was observed for the seismically-active volume of the crystalline rock at the depth of 2500-3500m.

Equation (5) provides scalar estimates of D only. Let us now assume, that D_{ij} is homogeneously distributed in the medium. When estimating the diffusivity under such an assumption we replace the complete heterogeneous seismically-active rock volume by an effective homogeneous anisotropic poroelastic fluid-saturated medium. The permeability tensor of this effective medium is the permeability tensor of the heterogeneous rock upscaled to the characteristic size of the seismically-active region.

Performing very similar consideration as in Shapiro et al. (1997), but now using equation 2) in a scaled principal coordinate system, the following equation for the triggering front can be obtained for anisotropic media (Shapiro et al., 1999):

$$r = \sqrt{\frac{4\pi t}{\mathbf{n}^T \mathbf{D}^{-1} \mathbf{n}}}. \quad (6)$$

T denotes that the matrix (vector) is transposed, $\mathbf{n} = \mathbf{r}/|\mathbf{r}|$ and \mathbf{D}^{-1} is the inverse of \mathbf{D} .

Group-velocity surface of anisotropic slow waves

To gain more insight into the physical nature of the triggering-front surface (eq. 6) we consider solutions of the anisotropic diffusion equation (2) in the form of homogeneous plane waves:

$$e^{(ik_j x_j - i\omega t)}. \quad (7)$$

Because we look for homogeneous waves (i.e. the real and imaginary parts of the wave vector are parallel) we can define a unit vector \mathbf{e} in the direction of the wave vector \mathbf{k} :

$$\mathbf{k} = \mathbf{e} (a + ib) = \mathbf{e} k, \quad (8)$$

where a and b are real numbers and k is a complex one. Substituting equation (7) into the diffusion equation (2) we obtain the following dispersion relationship characterizing the low-frequency propagation of slow waves:

$$\omega = -iD_{lm}k_l k_m = -iD_{lm}e_l e_m k^2. \quad (9)$$

This equation gives

$$|k^2| = \frac{|\omega|}{D_{gs}e_g e_s}. \quad (10)$$

The dispersion equation provides us with the following group velocity of anisotropic low-frequency slow waves (see the definition of the group velocity in Landau and Lifshitz (1984)):

$$V_j^{gr} = \frac{\partial \omega}{\partial k_j} = -iD_{lm}(k_l\delta_{mj} + k_m\delta_{lj}) = -2iD_{lj}k_l = -2iD_{lj}e_l k, \quad (11)$$

This gives the following absolute value of the group velocity:

$$\begin{aligned} |V^{gr}|^2 &= V_j^{gr*}V_j^{gr} \\ &= -2iD_{lj}e_l k \cdot 2iD_{mj}e_m k^* \\ &= 4D_{lj}D_{mj}e_l e_m |k|^2 \\ &= 4D_{lj}D_{mj}e_l e_m \frac{|\omega|}{D_{gs}e_g e_s} \\ &= 4|\omega| \frac{\mathbf{e}^T \mathbf{D} \mathbf{D} \mathbf{e}}{\mathbf{e}^T \mathbf{D} \mathbf{e}}, \end{aligned} \quad (12)$$

In turn, eq. (11) shows that the direction of the group velocity is defined by a unit vector \mathbf{e}^{gr} with the components:

$$e_j^{gr} = D_{lj}e_l / \sqrt{D_{gm}e_g D_{sm}e_s}. \quad (13)$$

Changing now the notations: $\mathbf{e}^{gr} = \mathbf{n}$ we finally arrive at the following result:

$$|V^{gr}| = \sqrt{\frac{4|\omega|}{\mathbf{n}^T \mathbf{D}^- \mathbf{n}}}. \quad (14)$$

A comparison of equations (6) and (14) shows that the triggering front has the same spatial form as the group-velocity surface of anisotropic slow waves. Physically this means that in the case of a point injection source triggering fronts in anisotropic rocks propagate like heat fronts or light fronts in anisotropic crystals.

Inversion for the global diffusivity and permeability tensors

Recently a new approach for estimating the global hydraulic diffusivity tensor was proposed by Shapiro et al. The new algorithm is based on a transformation of the microseismic events into a scaled coordinate system. Here all events must lie within an envelope ellipsoid whose half axes represent the orientation and magnitude of the diffusivity. For further details, the application to different data sets and the determination of the global permeability tensors see "J. Rindschwendter: Estimating the Global Permeability Tensor using Hydraulically Induced Seismicity - Implementation of a new Algorithm" within this volume.

TRIGGERING FRONTS IN HETEROGENEOUS MEDIA

For details on the 3-D mapping of hydraulic diffusivity we refer to further publications (see e.g. Shapiro, WIT Report no. 3, 53-63). To demonstrate the idea of the approach we just illustrate the main points of the method in the following. Figure 2 shows a view of the microseismic cloud collected during the Soultz experiment 1993. For each event the color shows its occurrence time in respect to the start time of the injection. With a subdivision of the space to a number of 3-D cells we can define an arrival time of the triggering front into each of these cells. Figure 2 also shows such a triggering front for the arrival times of 100h. Such a surface can be constructed for any arrival time presented in microseismic data. The time evolution of the triggering surface, i.e., the triggering front propagation can be characterized. In a heterogeneous porous medium the propagation of the triggering front is determined by its heterogeneously distributed velocity. Given the triggering front positions for different arrival times, the 3-D distribution of the propagation velocity can be reconstructed. In turn, the hydraulic diffusivity is directly related to this velocity.

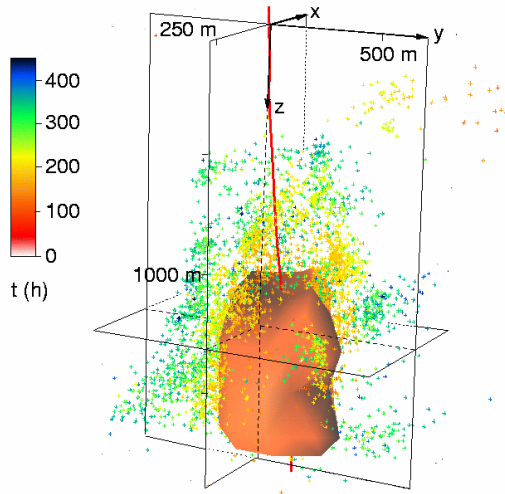


Figure 2: A perspective projection of the 3-D distribution of microseismic events registered during the Soultz-sous-Forets experiment: Borehole GPK1, September 1-22, 1993. The color corresponds to the event occurrence time. The axes X,Y and Z point to the East, the North and the earth surface, respectively. The surface shown is the triggering front of microseismicity for the arrival time of 100h. The vertical and horizontal scales of the Figure are equal.

Triggering fronts for the case of a quasi-harmonic pressure perturbation

In the following we shall consider relaxation of a harmonic component of a pressure perturbation. By analogy with (4) we will look for the solution of (1) in a similar form:

$$p(\mathbf{r}, t) = p_0(\mathbf{r}) e^{-i\omega t} \exp [\sqrt{\omega} \tau(\mathbf{r})], \quad (15)$$

We also will assume that $p_0(\mathbf{r})$, $\tau(\mathbf{r})$ and $D_{ij}(\mathbf{r})$ are functions slowly changing with \mathbf{r} .

Substituting (15) into (1), accepting ω as a large parameter and keeping only terms with largest powers of ω (these are terms of the order $O(\omega)$; the other terms, which are of the orders $O(\omega^0)$ and $O(\omega^{1/2})$ are neglected) we obtain the following equation:

$$-i = D_{ij} \frac{\partial \tau}{\partial x_i} \frac{\partial \tau}{\partial x_j}. \quad (16)$$

Considering again the homogeneous-medium solution (4) we conclude that the frequency-independent quantity τ is related to the frequency-dependent phase travel time T as follows:

$$\tau = (i - 1) \sqrt{\omega} T. \quad (17)$$

Note, that in turn $T \propto 1/\sqrt{\omega}$. Substituting equation (17) into equation (16) we obtain:

$$1 = 2\omega D_{ij} \frac{\partial T}{\partial x_i} \frac{\partial T}{\partial x_j}. \quad (18)$$

In the case of an isotropic poroelastic medium this equation is reduced to the following one:

$$|\nabla T|^2 = \frac{1}{2\omega D}. \quad (19)$$

Thus, we have obtained a standard eikonal equation. The right hand part of this equation is the squared slowness of the slow wave. One can show (Cerveny, 1985) that equation (19) is equivalent to the Fermat's principle which ensures the minimum time (stationary time) signal propagation between two points of the medium. Due to equation (17) the minimum travel time corresponds to the minimum attenuation of the signal. Thus, in this sense, equation (19) describes the minimum-time maximum-energy front configuration.

Triggering fronts in the case of a step-function like pressure perturbation

We now return to a more realistic situation, where the pressure perturbation can be roughly approximated by a step function in the source point.

In the previous section we derived an equation for the triggering time $T(\mathbf{r})$ of a harmonic pressure perturbation. Using this equation we shall derive another one, which will describe the triggering time $t(\mathbf{r})$ of a step-function pressure perturbation. From our earlier discussion we know, that the triggering time t roughly corresponds to the frequency

$$\omega_0 = 2\pi/t. \quad (20)$$

Thus,

$$T|_{\omega=\omega_0} = t. \quad (21)$$

From the other hand, we know that generally $T(\omega) \propto \sqrt{1/\omega}$. Now we can also use this relationship to compute T at the frequency ω_0 , if T is known at any arbitrary frequency ω :

$$t = T(\omega_0) = T(\omega) \sqrt{\frac{\omega}{\omega_0}}. \quad (22)$$

Using this equation and equation (20) we obtain:

$$T(\omega) = \sqrt{\frac{2\pi t}{\omega}}. \quad (23)$$

Substituting this equation into equations for T of the previous section we obtain the following results. In the general case of an anisotropic heterogeneous poroelastic medium

$$t = \pi D_{ij} \frac{\partial t}{\partial x_i} \frac{\partial t}{\partial x_j}. \quad (24)$$

In the case of an isotropic poroelastic medium this equation is reduced to the following one:

$$D = \frac{t}{\pi |\nabla t|^2}. \quad (25)$$

Inversion for the permeability of heterogeneous media

In the case of an isotropic poroelastic medium equation (25) can be directly used to reconstruct the 3-D heterogeneous field of the hydraulic diffusivity. In turn, equation (24) shows, that in the case of an anisotropic medium it is impossible to reconstruct a 3-D distribution of the diffusivity tensor. The only possibility is the following. Let us assume that the orientation and the principal components proportion is constant in the medium. Then, the tensor of hydraulic diffusivity can be expressed as

$$D_{ij}(\mathbf{r}) = d(\mathbf{r}) \xi_{ij}, \quad (26)$$

where ξ_{ij} is a nondimensional constant tensor of the same orientation and principal-component proportion as the diffusivity tensor, and d is the heterogeneously distributed magnitude of this tensor. This tensor can be found using the global SBRC estimate of

the hydraulic diffusivity as was mentioned above. Then, the quantity d can be directly computed as follows:

$$d = \frac{t}{\pi \xi_{ij} \frac{\partial t}{\partial x_i} \frac{\partial t}{\partial x_j}}. \quad (27)$$

Let us finally consider an example of application of the method. Figure 3 shows the reconstructed hydraulic diffusivity for Soultz-1993 data set according to equation (25). From the other hand assuming, that the tensor ξ_{ij} has the same orientation and principal-component proportion as the diffusivity tensor given in equation (16) of Shapiro et al. (1999), equation (27) can be applied to obtain the diffusivity-tensor magnitude.

It is interesting to note that there is no significant difference between the representation of the isotropic and anisotropic variant of the method. They both show larger diffusivity in the upper part of the medium then of the lower one. In addition, a high permeable channel leading to the upper right-hand part of the medium is visible in the reconstructed hydraulic diffusivity. This is in good agreement with Figure 2, which shows a number of early events in the upper right-hand corner of the rock volume.

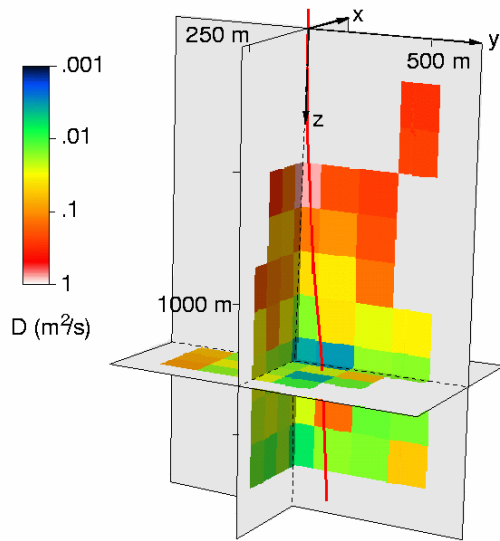


Figure 3: An example of the hydraulic diffusivity reconstruction in 3-D for the Soultz-1993 data set. For the inversion isotropic variant of the method has been used. The diffusivity is given in the logarithmic scale. It changes between 0.001 and $1.0 \text{ m}^2/\text{s}$. Light gray corresponds to cells with no diffusivity value resolved. The geometry corresponds to that given in Figure 2.

DISCUSSION

The main limitations of the extension of the SBRC to the case of heterogeneous media proposed here are apparently related to the validity range of equation (16). Roughly they can be formulated from the following consideration of the right hand part of equation (1) in a 1-D medium:

$$\frac{\partial}{\partial x} \left[D \frac{\partial p}{\partial x} \right] = \frac{\partial D}{\partial x} \frac{\partial p}{\partial x} + D \frac{\partial^2 p}{\partial x^2} \quad (28)$$

Our approach is expected to be valid if the following inequality is satisfied:

$$\left| \frac{\partial D}{\partial x} \frac{\partial p}{\partial x} \right| / \left| D \frac{\partial^2 p}{\partial x^2} \right| \ll 1 \quad (29)$$

This can be roughly reduced to the following: $\left| \frac{\partial D}{\partial x} \right| / |Dk| \ll 1$, where k is the wave number. Taking into account that approximately $|k|^2 = \omega/D$ we arrive at the following, rather simplified condition:

$$\frac{|\partial D / \partial x|^2}{D} < \omega. \quad (30)$$

This inequality relates the gradient of the hydraulic diffusivity and the frequency of the pressure perturbation. It is rather typical for the geometric optic approximation. It shows, that if the frequency is high enough and the medium heterogeneity is smooth the above approximation can be applied. In the case of the step-function like pressure perturbation the frequency corresponding to the triggering front is accepted to be $\omega = 2\pi/t$. Using the equation of the triggering front in homogeneous poroelastic media (5) the occurrence time of earlier events can be roughly approximated as $t \approx x^2/(4\pi D)$. Note, that x denotes the distance from the injection source. Thus, inequality (30) can be reduced to the following one

$$\frac{|\partial D / \partial x|}{D} \ll \frac{2\pi\sqrt{2}}{x}. \quad (31)$$

This condition is a rather restrictive one. In addition, it shows that the smaller distance x the higher is the resolution of the method.

In spite of the restrictive character of the inequalities above, we think that the geometric optic approximation is applicable to the propagation of microseismicity triggering fronts under rather common conditions. This is based on the causal nature of the triggering front definition. When considering the triggering front we are interested in a quickest possible configuration of the phase travel time surface for a given frequency. Thus, we are interested in kinematic aspects of the front propagation

only. The quickest possible configuration of the phase front is usually given by the Hamilton-Jacobi, i.e., eikonal equation. However, the conditions above necessarily take into account not only kinematic aspects of the front propagation but rather mainly dynamic aspects, i.e., amplitude of the pressure perturbation. In other words, the eikonal equation is usually valid in much broader domain of frequencies than those given by the inequalities above. Therefore, the method will give meaningful and useful results, at least semi qualitatively.

To verify the assertion that we are able to describe the diffusion process and the kinematics of the evolution of the triggering front in a heterogeneous medium by the use of the eikonal solution, we performed some numerical tests. We solved the parabolic differential equation of diffusion (1) in two spatial dimensions with the help of a finite elements method (FE) implemented in the MATLAB® computing environment. We calculated the time-dependent pressure variation through a medium where the diffusivity D varies smoothly in x direction with a Gaussian profile. It changes from a background value of $D = 0.5 \text{ m}^2/\text{s}$ to a minimal value of $D = 0.1 \text{ m}^2/\text{s}$ at the center. The half-width of this heterogeneity is approx. 200 m. The dimension of the computational mesh is 4000 m x 4000 m, and the source point is located at its center. As input signal we use a time-harmonic sinusoidal signal with a period of 400 h and 800 h respectively, multiplied with a boxcar function for the whole simulation time of 2400 h. The time increment in our simulations was $\Delta t \approx 3 \text{ h}$ while the elementary cell was of the order of 5 m x 5 m. We observe the pressure variation in a one dimensional section along the x-axis through the center of the model, where the source is located. In each point of observation we estimate the arrival time of the fourth resp. sixth zero-crossing of our quasi-periodic pressure signal. This was necessary to reduce the effects of the high-frequency components due to the finite character of the source signal. We compare this time with the corresponding theoretical eikonal solution

$$t = \int_0^R \frac{dr}{v(r)}. \quad (32)$$

Using the arrival time we also calculate the velocity v of the phase front at a given distance from the source point. Then we convert it into the diffusivity and compare the result with the exact diffusivity of the model. The diffusivity is calculated from the measured velocity of the phase front by

$$D(x) = \frac{v(x)^2}{4\pi f}, \quad (33)$$

where f is the dominant frequency of the source function (see eq. 4 and the comment below).

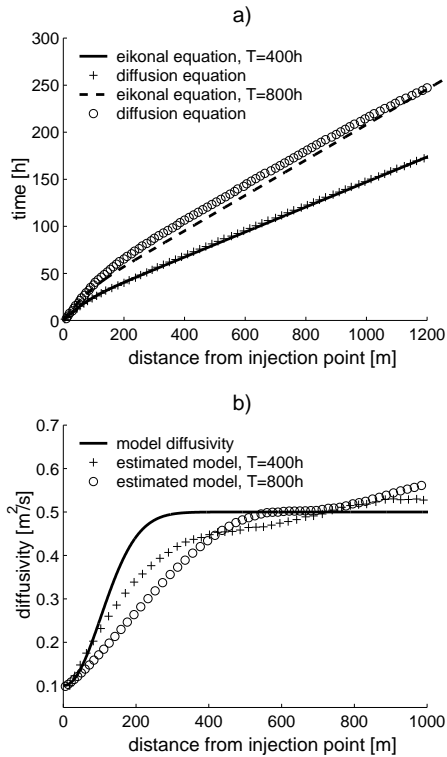


Figure 4: Comparison of eikonal equation and numerical diffusion models.

Reasonable agreement for both numerical experiments is found. In Fig. 4a the traveltimes are shown for the eikonal solution (32) and the numerical results. Fig. 4b shows the reconstructed diffusivity D at a given distance x in the medium. The good agreement between eikonal-predicted and numerically calculated traveltimes of the phase front in Fig. 4a is obvious. The small differences between the eikonal solution and numerical results at times $t < 50$ h can be explained with the relatively rough method we used to pick the phase front, i.e. the zero-crossing. The reconstructed diffusivity at a given distance in the medium also agrees very well with the exact value (see Fig. 4b). The differences at distances $x > 800\text{m}$ in Fig. 4b are caused mainly by influences of the prescribed boundary conditions, namely fixing the pressure to zero there (Dirichlet type). Thus the influences become larger at greater times and disturb the velocity of the triggering front measured during the numerical experiments. Differences between eikonal and exact numerical results are smaller for higher frequencies. This is obviously due to the fact, that the eikonal equation is a high frequency approximation, and therefore provides better results for smaller periods of the perturbation. In particular, the increasing difference between theoretical curve and the models in Fig. 4b is due to the fact that the region of inhomogeneity, i.e. increasing diffusivity, is smaller than the wavelengths used. The small differences observed between estimated and exact diffusivities indicate that the formal validity conditions (eqns. 29-30) are too restrictive.

CONCLUSIONS

We have developed a technique (SBRC) for reconstructing the permeability distribution in 3-D heterogeneous poroelastic media. For this we use the seismic emission (microseismicity) induced by a borehole-fluid injection. Usually, global estimates of permeabilities obtained by SBRC agree well with permeability estimates from independent hydraulic observations. Moreover, the global-estimation version of the SBRC provides the permeability tensor characterizing the reservoir-scale hydraulic properties of rocks. The processing of SBRC data for global estimates is based on the hypothesis that the triggering front of a hydraulic-induced microseismicity has the form of the group-velocity surface of anisotropic Biot slow waves. In this paper, we have further generalized the SBRC approach by using a geometrical-optic approximation for propagation of triggering fronts in heterogeneous media. We think, that results of such inversion for hydraulic properties of reservoirs can be used at least semi-quantitatively to characterize reservoirs. They can be very helpful as important constrains to reservoir modeling, or be starting models for more sophisticated inversions.

REFERENCES

- Audigane, P., February 2000, Caractérisation microsismique des massifs rocheux fracturés. Modélisation thermo-hydraulique. Application au concept géothermique de Soultz.: Ph.D. thesis, ENSG, INPL, Nancy, France.
- Biot, M. A., 1962, Mechanics of deformation and acoustic propagation in porous media: *Journal of Applied Physics*, **33**, 1482–1498.
- Cerveny, V., 1985, The application of ray tracing to the numerical modelling of seismic wavefields in complex structures: in *Seismic Shear Waves, Part A, Theory*, ed. G. Dohr, pages 1–124.
- Dyer, B., Juppe, A., Jones, R. H., Thomas, T., Willis-Richards, J., and Jaques, P., Microseismic Results from the European HDR Geothermal Project at Soultz-sous-Forêts, Alsace, France: CSM Associated Ltd, IR03/24, 1994.
- Fehler, M., House, L., Phillips, W. S., and Potter, R., 1998, A method to allow temporal variation of velocity in travel-time tomography using microearthquakes induced during hydraulic fracturing: *Tectonophysics*, **289**, 189–202.
- Landau, L. D., and Lifshitz, E. M., 1984, *Electrodynamics of continuous media*: Addison-Wesley, Reading, MA.
- Nur, A., and Booker, J., 1972, Aftershocks caused by pore fluid flow?: *Science*, **175**, 885–887.

Shapiro, S. A., and Müller, T., 1999, Seismic signatures of permeability in heterogeneous porous media: *Geophysics*, **64**, 99–103.

Shapiro, S. A., Huenges, E., and Borm, G., 1997, Estimating the crust permeability from fluid-injection-induced seismic emission at the KTB site: *Geophysical Journal International*, **131**, F15–F18.

Shapiro, S. A., Royer, J.-J., and Audigane, P., 1998, Estimating the Permeability from Fluid-Injection Induced Seismic Emission: Thimus J.-F., Abousleiman Y., Cheng A.H.-D., Coussy O. and E. Detournay, Eds., *Poromechanics*, 301–305.

Shapiro, S. A., Audigane, P., and Royer, J.-J., 1999, Large-scale in situ permeability tensor of rocks from induced microseismicity: *Geophysical Journal International*, **137**, 207–213.

Shapiro, S. A., Royer, J.-J., and Audigane, P., 2000, Reply to comment by F.H. Cornet on 'large-scale in situ permeability tensor of rocks from induced microseismicity': *Geophysical Journal International*, **140**, 470–473.

Talwani, P., and Acree, S., 1985, Pore pressure diffusion and the mechanism of reservoir-induced seismicity: *Pure appl. geophys.*, **122**, 947–965.

Zoback, M., and Harjes, H.-P., 1997, Injection induced earthquakes and the crustal stress at 9km depth at the ktb deep drilling site: *Journal of Geophysical Research*, **102:18**, 477–492.